Available online at www.sciencedirect.com
SCIENCE @ DIRECT®

Polymer 44 (2003) 3165–3171

polymer

www.elsevier.com/locate/polymer

Crosslinking in the melt of EVA using tetrafunctional silane: gel time from capillary rheometry

Yannick Goutille, Christian Carrot*, Jean-Charles Majeste, Frédéric Prochazka

Laboratoire de Rhéologie des Matières Plastiques, FRE CNRS 2396, Faculté des Sciences et Techniques, Université Jean Monnet,
23 Rue du Docteur Paul Michelon, 42023 Saint-Etienne Cedex 2, France

Received 5 November 2002; received in revised form 10 March 2003; accepted 14 March 2003

Abstract

Crosslinking of ethylene vinyl acetate (EVA) copolymers can be performed in the melt by use of a transesterification reaction using tetrapropoxysilane as a crosslinking agent and dibutyl tin oxide as a catalyst [Polymer 43 (2002) 6085]. Whether the kinetics of the reaction can be suitably controlled is an important point that must be answered before any processing method such as extrusion or injection molding is considered. This investigation was carried out in a capillary rheometer. Various stoichiometric ratio and processing temperatures were studied. Viscosity was measured during the reaction and the evolution of the flow curves with reaction time was calculated. Gel point under shear conditions was considered to be achieved at the appearance of a yield stress on the flow curves. It was shown that an excess of propoxy groups slows down the reaction kinetics but until 120 °C, the gelling time is longer than 8 minutes which is long enough for processing with conventional techniques.

Keywords: Ethylene vinyl acetate copolymer; Silane; Crosslinking

1. Introduction

EVA copolymers can be easily crosslinked for various purposes. Especially, after crosslinking, EVA can be used as an elastomer or as the elastomeric soft phase in TPV formulations including polyolefins as matrix. This reaction can be performed in the melt and in the early stage of the crosslinking reaction, both types of materials can be processed as conventional thermoplastics. Provided that the induction time before the gel formation is long enough, the processing by classical forming techniques such as extrusion or injection molding is possible. The high viscosity of the polymer makes the handling of the material very easy even before crosslinking for example for the making of profiles while such operations are not possible with low molecular weight organic liquids prior to crosslinking.

Crosslinking of ethylene vinyl acetate copolymers in the melt is usually performed by a free radical mechanism which needs the use of initiators such as organic peroxides, for example dicumyl peroxide [2–6] for hydrogen abstraction.

As for polyolefins, free radical grafting of functional monomers such acrylic acid or maleic anhydride followed by crosslinking with functional polymers [7,8], or free radical grafting of polyfunctional monomers such as vinylsilane [9] or triallyl cyanurate [10] followed by crosslinking can be carried out in the melt.

However, it has been shown for a long time that transesterification reactions can also be used for the same purpose preventing chain scission observed during free radical reactions. For example, co-crosslinking of EVA and ethylene methacrylate copolymers in presence of bibutyltinoxide (DBTO), which involves the coupling through an exchange of an ester with another ester, has been studied by Cassagnau et al. [11–13].

Recently a new exchange reaction between ester groups and alkoxysilane in presence of DBTO has been studied by Bounor-Legaré et al. [1] in the same team. Reactants such as tetraalkoxysilanes have been used in the temperature range between 100 and 180 °C. Tetramethoxysilane (TMOS) or tetraethoxysilane (TEOS) were reacted with model esters while TPOS was reacted with EVA. Crosslinking of EVA

---

* Corresponding author. Tel.: +33-4774-81555; fax: +33-4774-85126.
E-mail address: carrot@univ-st-etienne.fr (C. Carrot).

0032-3861/03/$ - see front matter © 2003 Elsevier Science Ltd. All rights reserved.
doi:10.1016/S0032-3861(03)00259-3

by tetrapropoxysilane (TPOS) using DBTO as a catalyst is a transesterification reaction and involves the exchange of acetate groups from EVA and propoxysilane groups from TPOS, all alkoxide groups being exchangeable.

Both a one step mechanism or two steps mechanism (grafting of the silane on EVA then crosslinking) have been evoked [1] to explain the crosslinking reaction according to the following scheme where two alkoxide groups are involved:

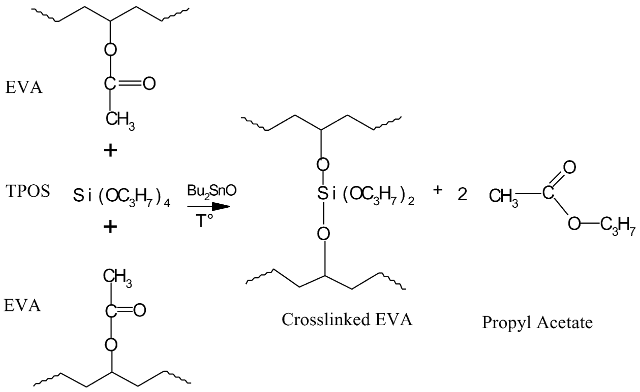

To be performed in the melt in a batch mixer or a twin screw extruder in the temperature and residence time range for the processing of EVA, these transesterification reactions require a suitable catalyst. The catalyst enables to obtain high yields at a lower temperature in a short time. DBTO has been many times quoted as an efficient catalyst system for exchange reaction between ester and alcohol in the melt [14–16], exchange reaction between ester and ester [11–13,17] and finally for exchange reaction between alkoxysilane and ester [1]. Indeed, the later studies all agree that DBTO first reacts with the ester groups and acts as a precursor of the real catalyst which is formed as a acyloxy–alcoxy distannoxane. The building of the catalyst in situ on the EVA polymer explains its dispersion and high activity [18,19].

Because, a precise knowledge of the kinetics of the reaction is necessary in order to avoid the crosslinking during the blending stage in the melt inside the extruder or during the filling of a mold, rheology and especially oscillatory experiments, have been used for this purpose by Cassagnau et al. in the case of various transesterification reaction involving EVA blends [1,11–13]. The present paper investigates the kinetics of the crosslinking reaction by means of capillary experiments which can be considered to be closer to the real processing situation because of the large strains involved.

2. Experimental section

2.1. Materials

Poly(ethylene-*co*-vinylacetate) (EVA) with a vinyl acetate weight content of 28% was supplied by Atochem in pelletized form (Evatane® 28 40). Tetrapropoxysilane (TPOS) in liquid form (Sigma-Aldrich, purity: 95%) and dibutyltin oxide (DBTO) in powder form (Sigma-Aldrich, purity: 98%) were used as received. The number average diameter of the catalyst powder was found to be 3.4 ± 0.5 μm, however it is worth mentioning that numerous agglomerates with larger sizes were observed and that the actual size may be significantly reduced during the blending stage.

2.2. Blends preparation

Because TPOS is strongly reactive with water, the components were kept in dried atmosphere or vacuum prior to use and between the experiments. Fresh blends were prepared just before the capillary rheometer experiments and never kept more than 8 h. The EVA copolymer was dried under vacuum during 24 h before use. Blending of the component was achieved in a Haake Rheocord mixer at 32 rpm at 50 °C. This temperature was chosen to ensure melting of the EVA and that the system remains unreacted during the blending stage.

Pure EVA (A0), non-reactive blends of EVA and TPOS (B1, B2) and reactive blends of EVA, TPOS with the catalyst DBTO (C1, C2) were prepared following the composition of Table 1. The total amount of material enables the filling of the chamber of the mixer. Blends B1–C1 and B2–C2 differ from the stoichiometry point of view. In blend B1 and C1, the ratio of acetate groups over propoxy groups [AV]/[OR] is 0.5 whereas it is 1 in the case of B2 and C2. For the reactive blends, the catalyst amount of 0.5 phr was chosen in order to have a reaction time which is compatible with that of the capillary experiment.

Half of the EVA and the DBTO were introduced in the mixer chamber and blended together until melting of EVA is achieved. This stage enables a good dispersion of the catalyst into the EVA matrix because of the friction of pellet and powder prior to melting. Half of the TPOS was slowly syringed in the chamber. Because TPOS is miscible with EVA, full absorption of TPOS is rapidly achieved. The process was repeated twice until the completion of the filling of the chamber. Then the components were mixed during 10 min. The molten blends were generally transparent at the end of the process. After crystallization, they were manually grinded with usual care to avoid moisture

Table 1
Blend composition

Reference	EVA (g)	TPOS (g)	DBTO (g)	[VA]/[OPr]
A0	50.4	0	0	–
B1	35.26	15.15	0	0.5
B2	41.48	8.91	0	1
C1	35.12	15.09	0.176	0.5
C2	41.31	8.88	0.207	1

absorption. The resulting blends were kept under vacuum at 40 °C.

2.3. Capillary experiments

The capillary experiments were performed on an Instron 3211 operating under controlled piston speed equipped with a flat entry cylindrical die (length: 60 mm, diameter: 1 mm). It was assumed that the length is large enough to avoid Bagley correction. The force on the piston was recorded using a 2000 kg load cell. The available volume of material in the rheometer chamber is approximately 12 cm^3. Measurements were carried out at 100, 120 and 140 °C. The rheometer temperature was controlled on three zones along the cylinder and within the die. Overheating in the capillary in the shearing conditions was calculated to be lower than 1.6 °C for the more viscous material and the difference of overheating between the samples never exceeds 0.6 °C.

The flow curve of EVA was measured at six different operating speeds in the usual way. The stability of the non-reactive blends was checked at 140 °C by extrusion at a low speed during more than an hour. In a similar way, the stability towards evaporation of the TPOS was checked. Thus, the flow curves of the B1 and B2 systems could be obtained as in the case of sample A0.

For the reactive blends, the measurements were performed at constant speed during at least 25 min after the feeding of the barrel. Four piston speeds (0.06, 0.2, 0.6, 2 cm/min) corresponding to apparent shear rates of 7.26, 24.2, 72.6, 242 s^{-1} were investigated. Considering the amount of material in the cylinder, the residence time can be varied on a large range. For the lowest temperature and the lowest piston speed (0.06 cm/min), it was possible to perform measurements during 45 min. However in the case of the highest speed, the amount of material in the cylinder was too small to enable continuous measurements. The extrusion was first initiated at 0.06 cm/min, then it was raised to the rate of interest and measurements were performed during a few seconds. After a while the piston speed was decreased again. The procedure was repeated until the cylinder was emptied. In these particular conditions the total experiment could last 25 min. Different sequences of tests were performed to check that such a procedure does not alter the kinetics of the reaction. The reproducibility of the results was fair and within the accuracy of the measuring cell. It should be mentioned that at high temperature the extrusion was often limited by the overloading of the load cell.

2.4. Characterization of the crosslinked products

The degree of crosslinking of the final products was estimated from the unsoluble fraction and from swelling measurements [1].

Because it has been checked that uncrosslinked EVA is perfectly soluble in toluene, the unsoluble fraction of crosslinked systems was measured according to the following procedure: 120 mg (m_0) of product was immersed in toluene during 15 days. The remaining solid was then filtered, dried under vacuum at 45 °C and weighted (m_2). The unsoluble fraction (w_u) is defined as the ratio of the mass of the remaining polymer to the initial mass:

$$w_u = m_2/m_0 \tag{1}$$

Swelling measurements were carried out on the previous samples. The samples were weighted after 15 days in toluene before (m_1) and after drying (m_2). The weight swelling ratio (S_w) can be defined as the ratio of the mass prior to drying to the mass of the dried sample (m_1/m_2) while the volume swelling ratio (S_v) is corrected from the density of toluene ($\rho_t = 0.865$ g/cm^3) and EVA ($\rho_{EVA} = 0.843$ g/cm^3) :

$$S_w = m_1/m_2 \tag{2a}$$

And

$$S_v = 1 + (S_w - 1)\rho_{EVA}/\rho_t \tag{2b}$$

3. Results

3.1. Non-reactive blends

The flow curves of samples A0, B1 and B2 were obtained at three different temperatures 100, 120 and 140 °C and are shown in Fig. 1a–c. All the samples display a classical behavior with a Newtonian plateau in the low shear rate range and a shear thinning behavior in the high shear rate zone. Time–temperature superposition was successfully applied as shown in Fig. 2. Time–temperature shift factors with respect to the temperature of 140 °C were calculated from the superimposition of the shear strain–stress curves on a single master curve at the reference temperature of 140 °C. The activation energies for the variation of the shift factors, or equivalently on the zero shear viscosity, at a reference temperature of 140 °C are given in Table 2 and decrease with the increasing content of TPOS. Indeed, because TPOS is miscible with EVA in the molten state, it lowers the glass transition temperature of EVA and thus induces an increase in the free volume which in turn causes a decrease of the activation energy. Nevertheless, it has been noted that blend B1 reaches the limit of miscibility of TPOS in EVA at room temperature.

Some experiments have been also performed on EVA containing 0.5 phr of DBTO without TPOS to check the

Table 2
Activation energy on the zero shear viscosity of the non-reactive samples

Sample	A0	B1	B2
Activation energy (kJ/mol)	47.4	34.1	41.5

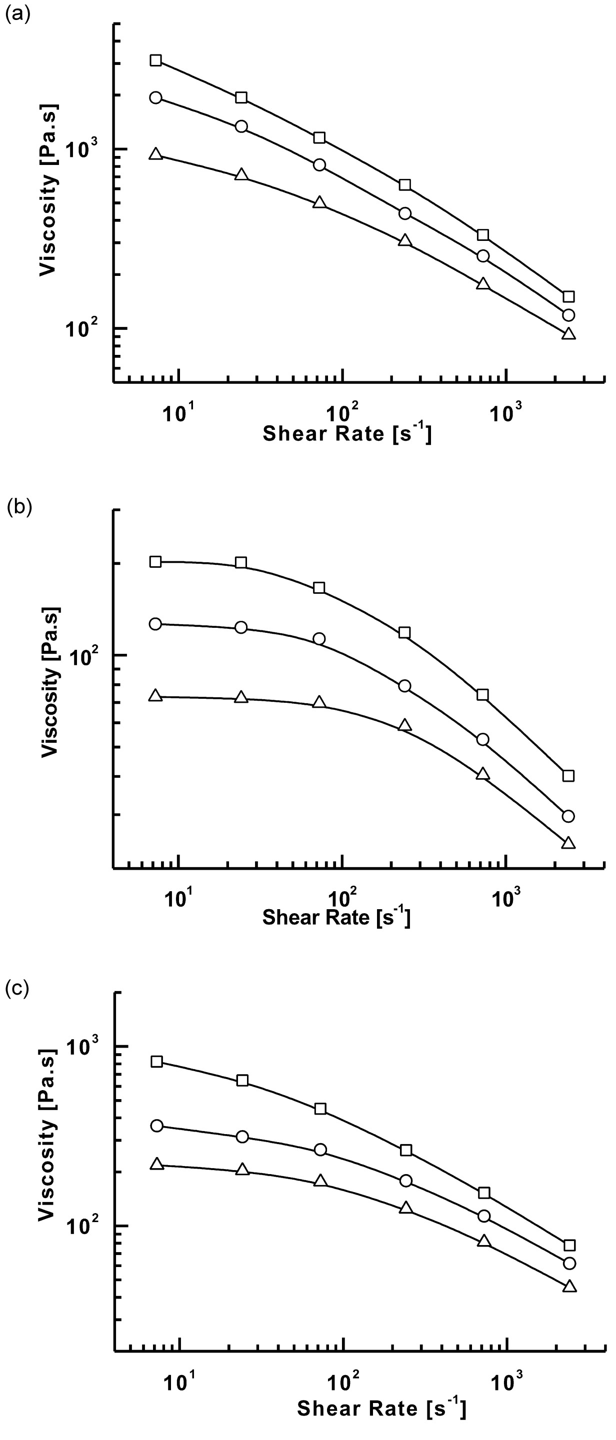

Fig. 1. (a) Flow curves (apparent shear viscosity versus apparent shear rate) of sample A0 (pure EVA) at 100 °C (□), 120 °C (○), 140 °C (△). (b) Flow curves (apparent shear viscosity versus apparent shear rate) of sample B1 (non-reactive blend) at 100 °C (□), 120 °C (○), 140 °C (△). (c) Flow curves (apparent shear viscosity versus apparent shear rate) of sample B2 (non-reactive blend) at 100 °C (□), 120 °C (○), 140 °C (△).

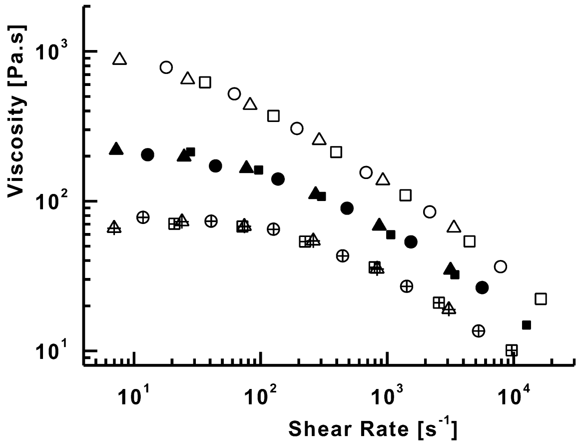

Fig. 2. Master flow curves (shear viscosity versus shear rate) of the non-reactive samples at 140 °C (open symbols: A0, crossed symbols: B1, filled symbols: B2).

possibility of a crosslinking of EVA in such conditions. At the highest temperature investigated (140 °C), it is shown that only a slight increase of the viscosity is observed. After 30 min, the increase in the viscosity is less than 3% and remains within the limit of accuracy of capillary measurements. After one hour, it reaches 15% but the flow behavior remains Newtonian which shows no evidence of crosslinking but could rather be attributed to branching.

3.2. Reactive blends: kinetics of the reaction

Fig. 3 shows a typical plot of the viscosity versus the residence time for blends C1 and C2 at 100 °C. Similar plots were obtained for the other temperatures. The plots shows that at 100 °C, after an induction time of about 15 min, the viscosity increases as expected due to the increase of the molecular weight. The sensitivity of the viscosity is much higher in the low shear rate zone because the zero shear viscosity is known to be very susceptible to changes in the structure of the polymers. During the induction time, bubbles are appearing inside the extrudate, then some gels are observed at the onset of the viscosity increase. Due to the non-miscibility of the catalyst with the polymer matrix, these primary gels are observed around the catalyst particles. Progressively, these gels extend to the whole

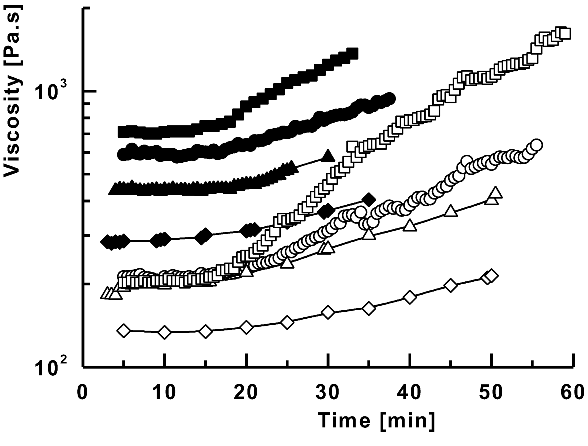

Fig. 3. Evolution of the apparent shear viscosity during the crosslinking of samples C1 (open symbols) and C2 (filled symbols) at 100 °C. The investigated apparent shear rates are: (□, ■): 7.26 s^{-1}, (○, ●): 24.2 s^{-1}, (△, ▲): 72.6 s^{-1} and (◇, ◆): 242 s^{-1}.

sample and some instabilities, namely melt fracture, can be observed. At last, especially for the high temperature where the conversion should be very high, the gel is broken under shear and the extrudate mainly consists in a very elastic polymer powder.

The comparison of the evolution of the crosslinking reaction at different temperatures is shown in Fig. 4 for the lowest shear rate under investigation (7.26 s^{-1}). The induction time decreases when the temperature increases and at 140 °C, the reaction starts immediately. The instability of the signal of the transducer at 120 and 140 °C is probably related to some slip of the very elastic material inside the die when the material is highly crosslinked.

4. Discussion

Points at defined constant time were extracted from Fig. 3 in order to draw the evolution of the flow curve of blend C1 and C2 as shown on Fig. 5a and b during the crosslinking reaction at 100 °C. The same procedure yields the plot of Fig. 6a and b for temperature 120 °C. The curve of non-reactive blends was also added for comparison. From a given reaction time, the flow curves display a change in their curvature. These curves were fitted using Eq. (3):

$$\eta(\dot{\gamma}) = \eta_0(1+(\lambda\dot{\gamma})^a)^{-1}\underline{+\tau_y/\dot{\gamma}} \qquad (3)$$

This equation is based on the Carreau-Yasuda [20,21] equation were η_0 is the zero-shear viscosity, λ is a characteristic time for the transition between the Newtonian and non-Newtonian behavior and a is related to the flow index at high shear rates.

The underlined term was added to take into account a yield effect, τ_y being the yield stress. Indeed, at the gel point the zero shear viscosity should diverge whereas a static modulus appears [22].

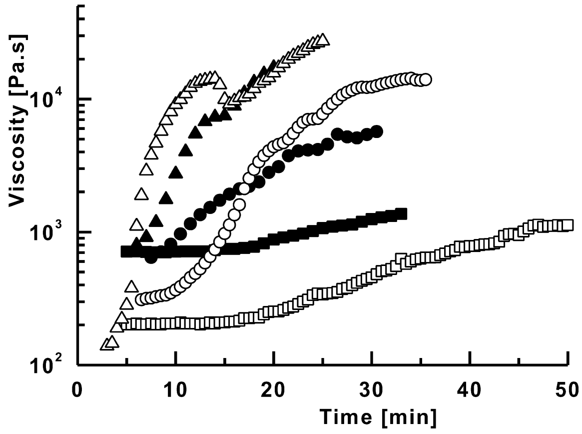

Fig. 4. Evolution of the apparent shear viscosity during the crosslinking of samples C1 (open symbols) and C2 (filled symbols) at the apparent shear rate 7.26 s^{-1}. The investigated temperatures are: (□, ■): 100 °C, (○, ●): 120 °C and (△, ▲): 140 °C.

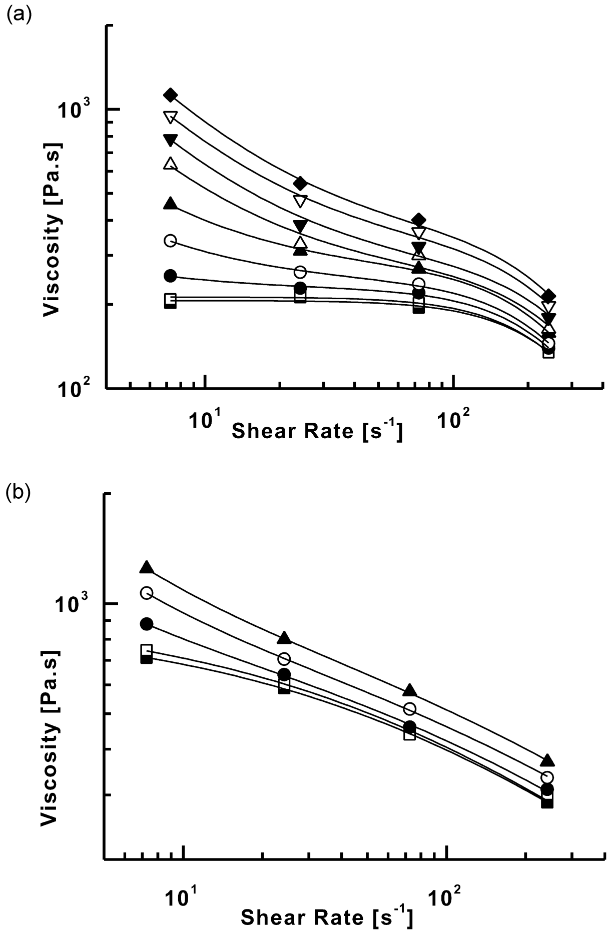

Fig. 5. (a) Evolution of the flow curve (apparent values) during the crosslinking of sample C1 at 100 °C and different reaction times: (■): 5 min, (□): 15 min, (●): 20 min, (○): 25 min, (▲): 30 min, (△): 35 min, (▼): 40 min, (▽): 45 min, (◆): 50 min. Line fit according to Eq. (3). (b) Evolution of the flow curve (apparent values) during the crosslinking of sample C2 at 100 °C and different reaction times: (■): 5 min, (□): 15 min, (●): 20 min, (○): 25 min, (▲): 30 min. Line fit according to Eq. (3).

Theoretical arguments can be developed to explain the form of this equation since before the gel, the material behaves like a viscoelastic liquid and after the gel, its behavior is a viscoelastic solid-like. Thus, before the gel the relaxation modulus can be written:

$$G(t) = \sum_i g_i \exp(-t/\lambda_i) \qquad (4a)$$

while after the gel it becomes:

$$G(t) = G_E + \sum_j g'_j \exp(-t/\lambda'_j) \qquad (4b)$$

where (λ_i, g_i) and (λ'_i, g'_i) are the relaxation modes (time and contribution to the modulus) for the viscoelastic medium before and after the gel while G_E is the static modulus [23].

Conversely, in the viscoelastic linear domain (low shear rates) in steady conditions, the stress can be written:

$$\tau = \dot{\gamma}\sum_i g_i\lambda_i = \dot{\gamma}\eta_0 \qquad (5a)$$

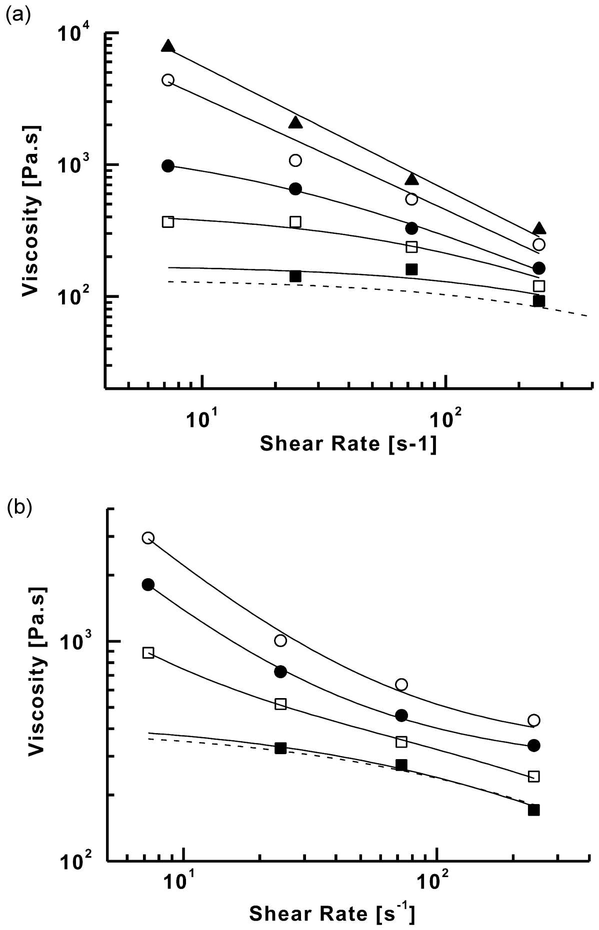

Fig. 6. (a) Evolution of the flow curve (apparent values) during the crosslinking of sample C1 at 120 °C and different reaction times: (■): 5 min, (□): 10 min, (●): 15 min, (○): 20 min, (▲): 25 min. Dashed line indicates the non-reactive blend B1. Line fit according to Eq. (3). (b) Evolution of the flow curve (apparent values) during the crosslinking of sample C2 at 120 °C and different reaction times: (■): 5 min, (□): 10 min, (●): 15 min, (○): 20 min. Dashed line indicates the non-reactive blend B2. Line fit according to Eq. (3).

before the gel, and

$$\tau = \gamma G_{\mathrm{E}} + \dot{\gamma}\sum_{j} g'_j \lambda'_j = \gamma G_{\mathrm{E}} + \dot{\gamma}\eta'_0 = \tau_{\mathrm{y}} + \dot{\gamma}\eta'_0 \qquad (5b)$$

after the gel. Eq. (5b) can finally be written in viscosity terms as:

$$\eta = \tau_{\mathrm{y}}/\dot{\gamma} + \eta'_0 \qquad (6)$$

It is clear that when the shear rate goes to zero, the characteristic divergence of the viscosity at the gel point may be equally and indistinctly obtained from a divergence of the viscosity or the appearance of a yield stress. As a consequence, a plot of the viscosity at low shear rate versus the reaction time yields the gel point when the viscosity goes to infinity or similarly a plot of the yield stress versus the reaction time yields the gel point at the appearance of a non-zero yield stress.

The viscosity plots of Figs. 5 and 6 were fitted with Eq. (3), without and with the yield term. The fit inducing the lower value of the chi-square value was used to draw the full line in Figs. 5 and 6. The values of the yield stress were plotted as a function of time for the systems under investigation (Fig. 7). The intercept point on the x-axis is considered to be the gel point.

Table 3 gives the values of the time for gelation in the different blends at various temperatures. It should be noted first that the gel time obtained through the capillary experiments are consistent with values obtained in Ref. [1] from the crossing of the storage and loss moduli in oscillatory shear flow experiments. It is worth reminding that according to Ref. [1], the gels under investigation show a −0.5 power dependence of the relaxation modulus which explain that the crossing of the moduli is characteristic of the gel point. With the same stoichiometry and catalyst content, the gel point for experiments at 120 °C is found to be 7.9 min whereas it is 4.8 min in Ref. [1]. The difference could certainly be attributed to a strain effect in the steady shear conditions.

Table 3 also shows that a change in the stoichiometry from stoichiometric conditions to an excess of propoxy groups slows down the reaction kinetics. This appears to be surprising since it would be in contradiction with the general kinetic laws of chemical reactions, however this is only true if the crosslinking reaction proceeds in a single step mechanisms with a single kinetic constant. If the overall reaction proceeds in a two steps mechanism, grafting then crosslinking, the gel which is governed by the crosslinking reaction is delayed because an excess of propoxy groups favors first grafting instead of crosslinking.

However, Table 4 shows from results on the state of crosslinking of the systems in the end of the reaction carried out in a batch mixer that for these stoichiometric ratio, the crosslinking density is only slightly affected. Only experiments involving large excess of ester groups ([VA]/[OPr] = 5 or 10) show that the crosslinking density is decreasing significantly.

As expected, the increase in the temperature of 20 °C

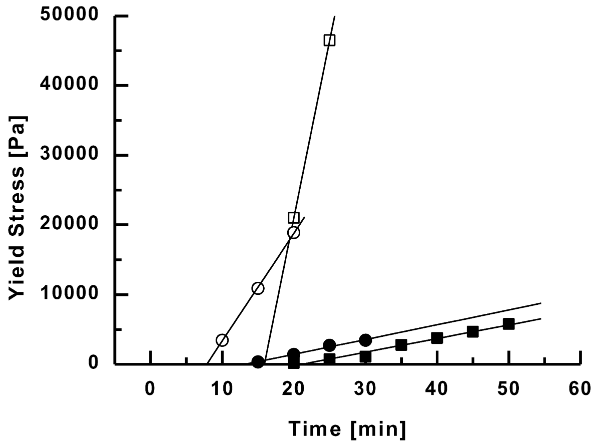

Fig. 7. Yield stress calculated from Eq. (3), (■): C1, 100 °C, (□): C1, 120 °C, (●): C2, 100 °C, (○): C2, 120 °C.

Table 3
Gel points from the onset of a yield stress

Reference	Temperature (°C)	Gel point (min)
C1	100	21.2
	120	15.9
C2	100	13.2
	120	7.9

Table 4
Unsoluble content and swelling ratio of some final products in various stoichiometric conditions

[VA]/[OPr]	w_u (%)	S_w	S_v
0.5 (Blend C1)	98.0	2.5	2.7
1 (Blend C2)	97.9	2.6	2.7
5	92.0	4.7	5.0
10	83.7	10.3	11.2

from 100 to 120 °C makes the reaction faster, the gel appearing 5 min sooner whatever the stoichiometry of the blend is.

5. Conclusions

The kinetics of the crosslinking reaction of ethylene vinyl acetate copolymers by tetrapropoxysilane with dibutyltin oxide as a catalyst was studied in a capillary rheometer. Stoichiometric ratio [VA]/[OPr] of 0.5 and 1 were investigated at temperature from 100 to 140 °C. At 140 °C the reaction was shown to start immediately and to be too fast to envision the use of this reaction for the crosslinking of extruded or injection-molded items. However, at temperature lower than 120 °C, the gel time was found to be longer than 8 min which becomes suitable for these applications. The gel time was measured under shearing conditions. For this purpose the flow curves during the reaction were obtained indirectly from measurements along time at constant shear rates. These curves were modeled by an empirical equation that accounts for a yield stress. The onset of a yield stress was assumed to be the proof of a gel.

Despite these encouraging results, it is worth mentioning that the proposed experimental conditions lead to the formation of a high amount of volatile end-products (propyl acetate) and that this may be considered as a limiting factor for the processes under investigation. Indeed, injection molding in these conditions may require special design of the molding tools with vents or sintered walls for degassing capabilities. However, in the present study, these conditions were chosen for convenience and minimization of the volatile products could also be obtained by an optimized decrease of the TPOS content.

The other problem is related to the immiscibility of the DBTO with the reacting system which makes the dispersion of the precursor of the catalyst difficult. Because this parameter may influence the efficiency of the overall catalytic effect, the efficiency of the dispersion of the powder has to be improved especially by screw designing in the extrusion and injection processes.

Acknowledgements

The ‘Région Rhône-Alpes’ is gratefully acknowledged for its financial support to this work which is part of a joined project which was carried out in partnership with the UMR CNRS 5627 in Lyon.

References

[1] Bounor-Legaré V, Ferreira I, Verbois A, Cassagnau P, Michel M. Polymer 2002;43:6085–92.
[2] Thomas S, Kuriakose B, Gupta BR, De SK. Plast Rub Proc Appl 1986; 6:101–6.
[3] Ray I, Khatsgir D. Plast Rub Proc Appl 1994;22:305–14.
[4] Mishra S, Bajewa B, Chandra R. J Appl Polym Sci 1999;74:2756–63.
[5] Li F, Zhu W, Zhang X, Zhao C, Xu M. J Appl Polym Sci 1999;71: 1063–70.
[6] Tai HJ. Polym Engng Sci 1999;39:1577–83.
[7] Mishra JK, Das CK. J Matter Sci 2001;20:1877–9.
[8] Soares BG, Colombaretti RSC. J Appl Polym Sci 1999;72:1799–806.
[9] Wang G, Jiang P, Zhu Z, Yin J. J Appl Polym Sci 2002;85:2485–90.
[10] Tai HJ. Polymer 2001;42:5207–13.
[11] Cassagnau P, Bert M, Verney V, Michel A. Polym Engng Sci 1992; 35:998–1003.
[12] Cassagnau P, Bert M, Verney V, Michel A. Polymer 1993;34:124–31.
[13] Espinasse I, Cassagnau P, Bert M, Michel A. J Appl Polym Sci 1994; 54:2083–9.
[14] Hu GH, Sun YS, Lambla M. Makromol Chem 1993;194:665–75.
[15] Lambla M, Druz J, Bouilloux A. Polym Engng Sci 1987;27:1221–8.
[16] Kim PJ, White JL. J Appl Polym Sci 1994;54:33–45.
[17] Lacroix C, Bousmina M, Carreau PJ, Llauro MF, Petiaud R, Michel A. Polymer 1996;37:2949–56.
[18] Pesneau I, Gregoire M, Michel A. J Appl Polym Sci 2000;79: 1556–62.
[19] Espinasse I, Petiaud R, Llauro MF, Michel A. Int J Polym Anal Charact 1995;1:137–57.
[20] Carreau PL. Trans Soc Rheol 1972;16:99–127.
[21] Yasuda K, Armstrong RC, Cohen RE. Rheol Acta 1981;20:163–78.
[22] Daoud M. Prog React Kinet 1989;15:1–34.
[23] Ferry JD. Viscoelastic properties of polymers, 3rd ed. New York: Wiley; 1980.